# PIER C SYAH ALAM 2025

*by* Syah Alam FTI

# Close Quarters Permittivity Detection Based on Tagging Antenna Sensor for Solid Material Characterization

Syah Alam[1], Indra Surjati[1], R. Deiny Mardian[1], Lydia Sari[1], Ghatfan Daffin[1], Iznih[1], Zahriladha Zakaria[2], Leni Devera Asrar[2], Teguh Firmansyah[3]
[1]Department of Electrical Engineering, Universitas Trisakti, West Jakarta, Indonesia, 11440
[2]Faculty of Electronic and Computer Engineering and Technology, Universiti Teknikal Malaysia Melaka, Malaysia, 76100
[3]Department of Electrical Engineering, Universitas Sultan Ageng Tirtayasa, Banten, Indonesia, 42117
e-mail: Syah Alam / syah.alam@trisakti.ac.id

***Abstract*—This research proposes a tagging antenna sensor for permittivity detection of solid materials based on a close quarter approach. The sensor is proposed to operate at a frequency of 2.53 GHz using a single port resonator with a reflection coefficient ($S_{11}$) ≤ -10 dB. The sample is placed directly in the sensing area of the antenna sensor based on the concentration of the electric field. Permittivity detection is proposed based on the resonant frequency shift of the transmission coefficient ($S_{21}$) using interrogator antennas separated by a distance of (d) = 100 mm determined using the Fresnel region. Based on the measurement results, the antenna sensor has a high accuracy of 96% while the sensitivity and ΔF are 0.39% and 0.012 GHz respectively. Moreover, the sensitivity of proposed sensor still low due the low concentration of the electric field. Therefore, increasing the sensitivity of the antenna sensor can be recommended as further work such as combining the structure of single port resonator with another structure such as interdigital capacitor and artificial magnetic conductor (AMC). Finally, this research makes a significant contribution to the permittivity detection of solid materials with a close quarter approach to support real time and flexible measurements and can be recommended for several applications for the biomedical, pharmaceutical and material quality control industries.***

**Keywords**: ***antenna sensor, close quarters, tagging detection, solid materials, permittivity***

## I. Introduction

Material characterization is important to observe the performance and interaction of materials under certain conditions [1]. One of the parameters to determine material characterization is permittivity. Permittivity shows the ability of a material to store electrical energy that will interact with an electric field [2],[3]. The interaction between the electric field and the material can be observed based on perturbation theory where the energy stored in the material will perturb the electric field so that the resonance frequency will shift to a low frequency in line with an increase in the permittivity of the sample[4],[5].

Generally, the permittivity of samples is detected using commercial probe sensors, but they have limitations including complex structure, bulk and low accuracy [6],[7]. Microwave sensors are one device that can be recommended for detecting the permittivity of samples[8][9]. The advantages of microwave sensors include compact dimensions, high accuracy and high sensitivity[10],[11]. Previous work proposed permittivity detection of solid samples using microwave sensors using Split Ring Resonator (SRR)[12], Dual Split Ring Resonator (D-SRR) [13], Complementary Split Ring Resonator (CSRR) [14], T-resonator[15] and interdigital structure (IDC) [16]. However, detection is currently proposed to be performed directly using a resonator, which means it does not allow for reading detection with certain distance. Apart from that, the sensor proposed in previous work uses a resonator with two ports so it cannot function as an antenna for transmitting electromagnetic waves. Moreover, tagging detection can also be proposed using RFID based approaches. RF ID based permittivity sensor has the capability to detect permittivity of samples using horn antenna as interrogator. Generally, detection is determined based on RSSI parameter of designed sensor which is connected with RFID reader to capture interaction between sensor and sample[17]–[19]. However, the configuration of complex measurement equipment becomes limitation. In addition, detection result must be processed using RFID reader which has potential to produce high error rate. Therefore, microwave sensors that have detection capabilities at a certain distance are needed to support real-time and flexible measurements.

This work proposes an antenna sensor for permittivity detection of samples based on a close quarter approach. A microwave sensor is proposed based on a resonator with a single port operating at a frequency of 2.53 GHz with reflection coefficient ($S_{11}$) ≤ -10 dB. Solid material samples are placed in the sensing area of the antenna sensor which is determined based on the electric field concentration. Furthermore, the interrogator antenna is proposed to detect permittivity with a certain distance (d) based on the frequency shift of the transmission coefficient parameters ($S_{21}$) of the antenna sensor.

The main contribution of this work is producing an antenna sensor that has the capability for tagging detection using a close quarter approach based on frequency shift for solid material characterization. Finally, this research can be recommended for permittivity detection in solid materials in real time for several applications including biomedical, pharmaceutical and material quality control.

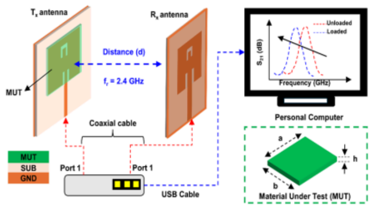


Figure 1. Proposed scenario for permittivity detection based on tagging antenna sensor

## II. Scenario for Close-Quarters Permittivity Detection Based on Tagging Antenna Sensor for Solid Materials

In this paper, the sensor antenna is designed to operate at a resonant frequency of 2.4 GHz using an FR-4 substrate with a permittivity of 4.3, a thickness of 1.6 mm and tan loss of 0.0265[12]. Validation and verification of the proposed sensor is carried out using a Vector Network Analyzer (VNA) which is connected directly to the antenna using a coaxial cable and a computer using a USB cable. The sample used is solid which has certain dimensions with length, width and thickness represented by *a, b* and *h*. The sample is placed in the sensing area of the sensor antenna which is connected with port 1 of the VNA as the transmitter ($T_x$). Next, permittivity detection of the sample is proposed using an interrogator antenna connected to port 2 of the VNA as a receiver (Rx). The distance of $T_x$ and $R_x$ is determined based on the Fresnel region of the proposed antenna which is represented by $d = 2D^2/\lambda$. The scenario of close quarter detection using the proposed sensor antenna is shown in **Figure 1**.

Permittivity detection is observed based on the frequency shift and response of the transmission coefficient parameter ($S_{21}$) of the interrogator antenna. Based on perturbation theory, the frequency of the resonator shifts lower in line with increasing permittivity of the sample placed in the sensing area of the antenna sensor.

The sensing area is defined by the region with maximum electric field concentration, as indicated by the E-field distribution. Furthermore, the sample placed on the sensor antenna which functions as $T_x$ will cause a frequency shift of the transmission coefficient on the interrogator antenna which functions as $R_x$. The correlation between frequency shift and permittivity change can be used to determine the permittivity of the sample using curve fitting based on polynomial equations.

## III. Method

### A. Development model of proposed antenna sensor

In this paper, the proposed antenna sensor is developed into three models represented by model 1, model 2 and model 3. Simulation and design of the sensor antenna is carried out using EM simulation with a resonance frequency of 2.4 GHz.

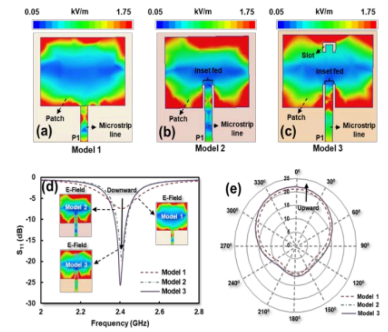


Figure 2. Development model and simulation result of proposed antenna at $f_r$ = 2.4 GHz; (a) E-field for model 1, (b) E-field for model 2, (c) E-field for model 3, (d) simulation of $S_{11}$, (e) simulation of radiation pattern.

Model 1 is shown with a microstrip antenna with a rectangular patch connected to port 1 using a microstrip line. Furthermore, inset feed and inverted U-shaped slots are proposed to improve the performance of the antennas represented by model 2 and model 3. The overall model development and electric field concentration of the proposed sensor antenna are shown in **Figure 2(a)**, **Figure 2(b)** and **Figure 2(c)**.

**Figure 2(a)**, **Figure 2(b)** and **Figure 2(c)** show that the proposed sensor antenna has a maximum electric field in the range of 0.05 - 1.75 kV/m at the center and edge of the patch at a resonance frequency of 2.4 GHz. Furthermore, the simulation results of $S_{11}$ with the addition of an inset feed and an inverted U-shaped slot are shown in **Figure 2 (d)**. Based on the simulation results, the $S_{11}$ of the proposed antenna with model 1 is still ≥ -10 dB, while for model 2 and model 3 antennas it is ≤ -10 dB. These findings indicate that the addition of an inset feed and an inverted U-shaped slot successfully improves the performance of the $S_{11}$ of the proposed antenna. In addition, the radiation pattern of the proposed antenna is shown in **Figure 2(e)** where model 3 has more optimal radiation compared to model 1 and model 2.

The dimensions of the sensor antenna are determined based on the resonant frequency and characteristics of the substrate used. The length and width of the antenna patch represented by $W_p$ and $L_p$ are determined based on the following equation[20]:

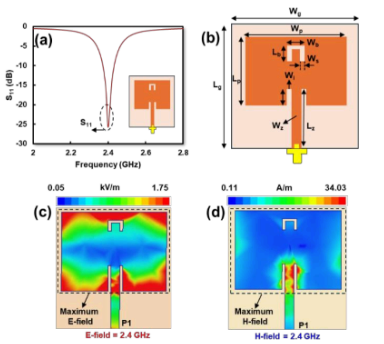


Figure 3. Simulation result and design of proposed antenna sensor; (a) $S_{11,}$ (b) structure of proposed sensor (c) E-field concentration at $f_r$ = 2.4 GHz, (d) H-field concentration at $f_r$ = 2.4 GHz

$$W_p = \frac{c}{2f_o\sqrt{\frac{(\varepsilon_r+1)}{2}}} \quad (1)$$

$$L_p = L_{eff} - \Delta_L \quad (2)$$

$$L_{eff} = \frac{c}{2f_o\sqrt{\varepsilon_{eff}}} \quad (3)$$

$$\varepsilon_{eff} = \frac{\varepsilon r+1}{2} + \frac{\varepsilon r-1}{2}[1+12\frac{h}{W_p}]^{-\frac{1}{2}} \quad (4)$$

$$\Delta_L = 0.412\frac{(\varepsilon_{reff}+0.3)(\frac{W_p}{h}+0.264)}{(\varepsilon_{reff}-0.258)(\frac{W_p}{h}+0.8)} \quad (5)$$

where $W_p$ and $L_p$ denote the patch's length and width, respectively, $f_o$ stands for the resonance frequency, $\varepsilon_r$ is the substrate's permittivity, $\varepsilon_{eff}$ indicates the substrate's effective permittivity at a specific resonance frequency, h signifies the substrate's thickness; and ΔL accounts for the fringing field's edge effect on the patch.

Additionally, microstrip lines are suggested to regulate the antenna's impedance and reflection coefficient represented by $W_z$. The dimensions of the microstrip line are significantly affected by the input impedance and the chosen resonant frequency. In this study, the input impedance is set at 50 ohms. The dimensions of the microstrip line can be calculated using the following equation[21].

$$W_z = \frac{2h}{\pi}\left\{B-1-\ln(2B-1)+\frac{\varepsilon_r-1}{2\varepsilon_r}\left[\ln(B-1)+0.39-\frac{0.61}{\varepsilon_r}\right]\right\} \quad (6)$$

$$B = \frac{60\pi^2}{Z_0\sqrt{\varepsilon_{eff}}} \quad (7)$$

In this context, $W_z$ represents the width of the microstrip line, $Z_0$ denotes the antenna impedance, and B is the impedance constant. The antenna's impedance is set at 50 Ω, consistent with the impedance of the connector employed.

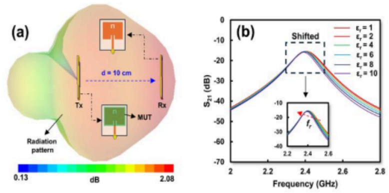


Figure 4. Simulation detection using antenna sensor; (a) tagging detection, (b) correlation between frequency and permittivity

Additionally, the length of the microstrip line ($L_z$) is ¼ $\lambda_g$, as determined by the following equation [22]:

$$L_z = {}^{1}/_{4}\,\lambda_g \quad (8)$$

$$\lambda_g = \frac{\lambda}{\varepsilon_{eff}} \quad (9)$$

Furthermore, $S_{11}$ of the proposed sensor antenna was ≤ -10 dB as shown in **Figure 3(a)** while the structure of the antenna is shown in **Figure 3(b)**. The overall dimensions of the sensor antenna structure are shown in **Table 1**.

Table 1. Dimension of proposed antenna sensor

| Parameters | Dimension (mm) |
|---|---|
| $W_g$ | 50 |
| $L_g$ | 50 |
| $W_p$ | 36 |
| $L_p$ | 28 |
| $W_z$ | 3 |
| $L_z$ | 15 |
| $W_b$ | 5 |
| $L_b$ | 4 |
| $W_i$ | 1 |
| $L_i$ | 9 |
| $W_s$ | 1 |

### *B. Simulation of permittivity detection using antenna sensor*

The concentration of the E-field from the antenna sensor is at the edge and center of the patch, while the H-field is in the microstrip channel gap as shown in **Figure 3(c)** and **Figure 3(d)**. However, the maximum concentration of the electric field is higher than the magnetic field so that the antenna characteristics are more capacitive. These findings indicate that areas with the highest E-field can be used as potential locations for sensing areas to detect the permittivity of samples. **Figure 4(a)** shows a scenario for tagging detection using the proposed antenna sensor where the Tx and Rx antennas are separated by a distance of *d* =10 cm determined based on the Fresnel region for a resonance frequency ($f_r$) of 2.4 GHz. Moreover, the permittivity of the sample placed in the $T_x$ antenna is detected by the $R_x$ antenna based on the frequency shift of the transmission coefficient ($S_{21}$) as shown in **Figure 4(b)**. Based on the simulation results, the frequency of the antenna sensor shifts to low frequencies in line with increasing permittivity of the sample.

### C. Simulation of tan delta detection using proposed sensor

Furthermore, the proposed sensor can also detect the change in dielectric losses of the sample based on the change in reflection coefficient ($S_{21}$) shown in **Figure 5(a).** The transmission coefficient of the proposed sensor moves to low along with the increase in dielectric loss of the sample in the range of 0 - 0.1. Based on the simulation results, the transmission coefficient shifts from -15.45 dB to -15.55 dB for the tan delta range of 0 - 0.1 as shown in **Figure 5(b)**. This finding indicates that the change in tan delta of the sample greatly affects the transmission coefficient of the proposed sensor.

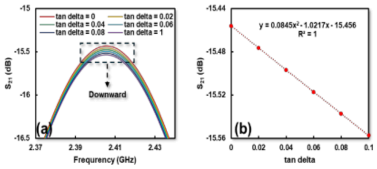

Figure 5. Simulation detection of tan delta with range of 0 – 0.1 using proposed sensor; (a) correlation resonance frequency with tan delta, (b) correlation between $S_{21}$ and tan delta

### D. Simulation of permittivity detection using antenna sensor with d = 5 cm – 10 cm

Furthermore, simulation with EM simulation is proposed to observe the performance of the proposed sensor against the distance between the sensor and the interrogator antenna represented by *d* for the range of 5 cm - 15 cm as shown in **Figure 6**.

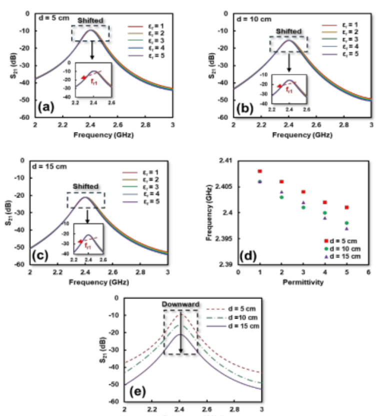

Figure 6. Simulation detection of tan delta with range of d = 5 cm – 15 cm using proposed sensor; (a) d = 5 cm, (b) d = 10 cm, (c) d = 15 cm, (d) correlation between distance with resonance frequency and permittivity of samples, (e) correlation between distance and $S_{21}$

Based on the simulation results, the sensor can detect the permittivity of the sample for the distance range d = 5 cm - 15 cm as shown in **Figure 6 (a)**, **Figure 6 (b)** and **Figure 6 (c)**. Furthermore, the correlation of the resonance frequency and permittivity is shown in **Figure 6 (d)** where the performance of the sensor is stable enough to detect the permittivity of the sample for the range d = 5 cm - 10 cm. The simulation results show that the resonance frequency shifts from 2.408 GHz to 2.401 GHz for *d* = 5 cm while for *d* = 10 cm it shifts from 2.406 GHz to 2.398 GHz and for *d* = 15 cm it shifts from 2.406 GHz to 2.397 GHz. Other findings show that the distance between the sensor and the interrogator antenna greatly affects the transmission coefficient ($S_{21}$) of the antenna where a long distance causes the transmission coefficient of the sensor to shift to low. The simulation results show that the $S_{21}$ of the proposed sensor shifts from -9.45 dB to -15.41 dB and -20.99 dB for the distance range d = 5 cm - 15 cm as shown in **Figure 6 (e)**. This finding indicates that the distance between the sensor and the interrogator antenna should be determined based on the fresnel region. Therefore, in this paper, the distance between the sensor and the antenna is determined based on the Fresnel region which is represented by $d = 2D^2/\lambda$.

## IV. Result And Discussion

### A. Measurement and verification

Measurements and verification of the proposed antenna sensor were carried out in the laboratory using a Vector Network Analyzer (VNA) with a frequency range of 2 - 2.8 GHz with a frequency step size of 0.001 GHz and an ambient temperature of $25^0$ C.

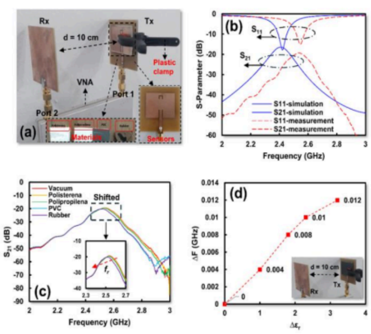

Figure 7. Measurement of proposed sensor; (a) setup for detection using tagging antenna sensor, (b) simulation and measurement result, (c) response of frequency with permittivity changes, (d) ΔF of proposed sensor.

Measurement setup for permittivity detection with a tagging antenna sensor with a distance of d = 10 cm where the sample is placed on the $T_x$ antenna which is connected to port 1 while for the $R_x$ antenna it is connected to port 2 as shown in **Figure 7(a)**. In this experiment, four types of solid materials are proposed as samples as follows: polystyrene, polypropylene, PVC and rubber. The permittivity of the sample was validated using a Keysight N1501A dielectric

Table 3. Comparison proposed antenna sensor with existing works

| Ref. | Method | $f_r$ (GHz) | Permittivity range | Samples | Sensing parameter | Sensing performance ΔF (GHz) | Sensing performance Acc. (%) | Sensing performance Sens. (%) | Tagging detection | Close quarter approach | Design complexity |
|---|---|---|---|---|---|---|---|---|---|---|---|
| [13] | Dual SRR | 2.27 | 1 – 4.3 | Solid | Freq. shift | 0.29 | 85% | 8.52 | No | No | Moderate |
| [14] | Nested CSRR | 3.37 | 1 – 4.3 | Solid | Freq. shift | 0.47 | 87% | 14.02 | No | No | High |
| [15] | T-ring resonator | 4.2 | 1 – 4.3 | Solid | Freq. shift | 0.18 | 95% | 5.45 | No | No | Moderate |
| [16] | Interdigital structure | 5.65 | 1 – 4.3 | Solid | Freq. shift | 0.17 | 98% | 3.25 | No | No | High |
| This work | Antenna with U -slot | 2.53 | 1 – 4.13 | Solid | Freq. shift | 0.012 | 96% | 0.39 | Yes | Yes | Low |

probe kit which was used as a reference to determine the permittivity of the sample using the proposed antenna sensor. The dimensions of the sample are adjusted to the location of the sensing area where the length, width and thickness is 36 mm x 28 mm x 1 mm respectively.

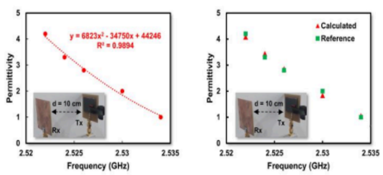


Figure 8. (a) Fitting curve for permittivity detection, (b) comparison permittivity from calculation and reference

Furthermore, to ensure accurate sample placement, plastic clamps were used to attach the sample to the surface of the antenna sensor. A comparison of simulation and measurement results from the antenna sensor for $S_{11}$ and $S_{21}$ is shown in **Figure 7(b)**.

Based on the measurement results, the sensor antenna experienced a frequency shift from 2.4 GHz to 2.53 GHz or a shift of 5.4 %. This result is due to the uncertainty of the fabrication process and the permittivity range of the FR4 substrate where $\varepsilon_r$ = 4.3 - 4.6. The correlation between the resonance frequency of the antenna sensor and changes in the permittivity of the sample is shown in **Figure 7(c)** where the resonance frequency shifts to a low frequency in line with the increase in the permittivity of the sample. The resonant frequency of the antenna sensor shifts from 2.534 GHz to 2.532 GHz for the four recommended samples with different permittivity as shown in **Figure 7(d)**. In this experiment, the reference frequency used was the unloaded condition (vacuum). Next, the range of frequency shift of the antenna sensor represented by ΔF is determined based on the following equation:

$$\Delta F = f_{unloaded} - f_{loaded}\ (GHz) \qquad (10)$$

where $f_{unloaded}$ shows the frequency of the antenna sensor when there is no material and $f_{loaded}$ is the frequency when the sample is placed on the antenna sensor. Based on the calculation using Equation (10), the maximum ΔF for the proposed antenna sensor is 0.012 GHz for the sample with the highest permittivity. Next, the permittivity of the sample is extracted based on fitting curve with a polynomial equation by observing the resonance frequency of the antenna sensor and the permittivity of the sample[23]. The correlation between the resonant frequency of the antenna and the permittivity of the sample is shown in **Figure 8(a)**. Based on **Figure 8(a)**, the correlation between permittivity and resonance frequency obtains a fitting curve with $R^2$ = 0.98. These results show that the equation obtained has high accuracy to determine the permittivity of samples. Furthermore, the permittivity of the sample can be determined using the following equation:

$$\varepsilon_r = 6823fr^2 - 34750fr + 4426 \qquad (11)$$

where $\varepsilon_r$ is the permittivity of the sample and $f_r$ is the resonance frequency of the antenna sensor for four types of materials with different permittivity. The accuracy of permittivity detection using an antenna sensor and comparison with detection using a sensor probe is shown in **Figure 8(b)** and **Table 2**.

Table 2. Comparison measurements from antenna sensor and probe sensors

| Samples | Permittivity | | Error (%) | Accuracy (%) |
|---|---|---|---|---|
| | Probe sensor | Antenna sensor | | |
| Vacuum | 1.05 | 1.02 | 2.7 | 97.31 |
| Polystyrene | 1.84 | 2.02 | 8.9 | 91.12 |
| Polypropylene | 2.85 | 2.82 | 1.1 | 98.85 |
| PVC | 3.44 | 3.32 | 3.6 | 96.38 |
| Rubber | 4.08 | 4.12 | 0.9 | 99.09 |

**Table 2** shows that the proposed antenna sensor has high accuracy for permittivity detection of the four solid materials with a range of 91% - 99%. Moreover, errors from measurement process arise from multiple sources, including calibration inaccuracies, environmental factors, and sensor design limitations. To minimize these errors, advanced calibration techniques, shielding from environmental interference, and improved sensor designs incorporating robust signal processing methods are essential.

In addition, the sensitivity (S) of the antenna sensor can be determined based on the following equation[23]:

$$S = \frac{\Delta F}{\Delta \varepsilon_r} \times 100\% = \frac{f_{loaded} - f_{unloaded}}{\varepsilon_r\ samples - \varepsilon_r\ vacuum} \times 100\% \qquad (12)$$

where $\Delta F$ is the difference between the unloaded frequency and the loaded frequency of the sensor antenna for each sample, while $\Delta\varepsilon_r$ is the difference between the sample permittivity and the vacuum condition where $\varepsilon_r = 1$ as a reference. Based on the calculation results using Equation (12), the sensitivity of the proposed antenna sensor is 0.39% with a permittivity range of 1.02 - 4.12. Therefore, the proposed antenna sensor can be recommended for detecting the permittivity of solid materials with high accuracy.

Furthermore, validation of this work was carried out by comparing the performance of the proposed antenna sensor with the microwave sensor proposed in previous work as shown in **Table 3**. The performance of the sensors compared included resonance frequency, sample type, permittivity range, accuracy, sensitivity and capability for tagging detection with a close quarter approach.

Previous work [13][14][15][16] proposed microwave sensors for permittivity detection of solid materials using Dual SRR, Nested SRR, T-ring resonator and interdigital structure. However, the proposed work is not capable of tagging detection over a certain distance and the structure is more complex to fabricate. **Table 3** shows that the main contribution of this work is producing an antenna sensor that has the capability for tagging detection using a close quarter approach based on frequency shift for solid material characterization. Moreover, the proposed antenna sensor has a high accuracy of 96% for the permittivity range 1 - 4.13. However, the sensitivity of the antenna sensor is still small because the E-field is not optimally concentrated. Therefore, increasing the sensitivity of the antenna sensor can be recommended as further work such as combining the structure of single port resonator with interdigital capacitor (IDC) structures [24] or using artificial magnetic coupled (AMC) as sensing area with high concentrations of electric field[25]. Finally, the proposed tagging permittivity sensors have a wide range of real-world applications, particularly in material identification, quality control, and environmental monitoring. These sensors utilize changes in permittivity to detect and differentiate materials in industries such as agriculture, food processing, and biomedical sensing. For instance, in agriculture, tagging permittivity sensors can monitor soil moisture content, ensuring optimal irrigation management. In the food industry, they help assess the freshness and composition of packaged goods by detecting changes in dielectric properties. In biomedical applications, these sensors can be integrated into wearable devices to monitor physiological parameters such as hydration levels and tissue properties.

## V. Conclusion

This research has succeeded in designing and realizing an antenna sensor that operates at a resonant frequency of 2.53 GHz for permittivity detection of solid materials using a close quarter approach. Permittivity is detected based on the frequency shift of the transmission coefficient of the sensor antenna and interrogator antenna which are separated by a distance (d) = 100 mm. The measurement results show that the antenna sensor has a high accuracy of 96% with a sensitivity of 0.39% and a $\Delta F$ of 0.012 GHz for a permittivity range of 1 - 4.13. These findings show that the proposed antenna sensor has high performance and can be recommended for real time measurements in the biomedical, pharmaceutical and material quality control industries.

## Reference


[1] R. A. Alahnomi *et al.*, "Review of Recent Microwave Planar Resonator-Based Sensors :," *Sens. Rev.*, vol. 2267, no. 21, pp. 1–38, 2021.

[2] J. Yeo and J. I. Lee, "High-sensitivity microwave sensor based on an interdigital-capacitor-shaped defected ground structure for permittivity characterization," *Sensors (Switzerland)*, vol. 19, no. 3, 2019, doi: 10.3390/s19030498.

[3] S. Lim, C. Y. Kim, and S. Hong, "Simultaneous Measurement of Thickness and Permittivity by Means of the Resonant Frequency Fitting of a Microstrip Line Ring Resonator," *IEEE Microw. Wirel. Components Lett.*, vol. 28, no. 6, pp. 539–541, 2018, doi: 10.1109/LMWC.2018.2833202.

[4] R. A. Alahnomi, Z. Zakaria, E. Ruslan, S. R. Ab Rashid, and A. A. Mohd Bahar, "High-Q sensor based on symmetrical split ring resonator with spurlines for solids material detection," *IEEE Sens. J.*, vol. 17, no. 9, pp. 2766–2775, 2017, doi: 10.1109/JSEN.2017.2682266.

[5] A. A. Mohd Bahar, Z. Zakaria, M. K. Md. Arshad, A. A. M. Isa, Y. Dasril, and R. A. Alahnomi, "Real Time Microwave Biochemical Sensor Based on Circular SIW Approach for Aqueous Dielectric Detection," *Sci. Rep.*, vol. 9, no. 1, pp. 1–12, 2019, doi: 10.1038/s41598-019-41702-3.

[6] E. M. Cheng *et al.*, "Reflection and dielectric measurement for salinity of water using microstrip loop antenna and dielectric probe," *Int. J. GEOMATE*, vol. 11, no. 2, pp. 2335–2340, 2016, doi: 10.21660/2016.24.1168.

[7] A. Mortari and L. Lorenzelli, "Recent sensing technologies for pathogen detection in milk: A review," *Biosens. Bioelectron.*, vol. 60, pp. 8–21, 2014, doi: 10.1016/j.bios.2014.03.063.

[8] J. G. D. Oliveira, J. G. D. Junior, E. N. M. G. Pinto, V. P. S. Neto, and A. G. D'Assunção, "A new planar microwave sensor for building materials complex permittivity characterization," *Sensors (Switzerland)*, vol. 20, no. 21, pp. 1–15, 2020, doi: 10.3390/s20216328.

[9] S. Alam, Z. Zakaria, I. Surjati, N. A. Shairi, M. Alaydrus, and T. Firmansyah, "Integrated Microwave Sensor and Antenna Sensor Based on Dual T-Shaped Resonator Structures for Contact and Noncontact Characterization of Solid Material," *IEEE Sens. J.*, vol. 23, no. 12, pp. 13010–13018, 2023, doi: 10.1109/JSEN.2023.3273008.

[10] S. Aiswarya, S. K. Menon, M. Donelli, and L. Meenu, "Development of a microwave sensor for solid and liquid substances based on closed loop resonator," *Sensors*, vol. 21, no. 24, pp. 1–34, 2021, doi: 10.3390/s21248506.

[11] S. Alam *et al.*, "UHF-Band Solid Sensor Based on Tweaking Electric Field Coupled Resonator for Material Characterization," *Prog. Electromagn. Res. M*, vol. 126, no. February, pp. 11–18, 2024, doi: 10.2528/PIERM24020201.

[12] A. Armghan, T. M. Alanazi, A. Altaf, and T. Haq, "Characterization of Dielectric Substrates Using Dual Band Microwave Sensor," *IEEE Access*, vol. 9, pp. 62779–62787, 2021, doi: 10.1109/ACCESS.2021.3075246.

[13] A. J. A. Al-Gburi, Z. Zakaria, I. M. Ibrahim, R. S. Aswir, and S. Alam, "Solid Characterization Utilizing Planar Microwave Resonator Sensor," *Appl. Comput. Electromagn. Soc. J.*, vol. 37, no. 2, pp. 222–228, 2022, doi: 10.13052/2022.ACES.J.370211.

[14] N. A. Rahman *et al.*, "High quality factor using nested complementary split ring resonator for dielectric properties of solids sample," *Appl. Comput. Electromagn. Soc. J.*, vol. 35, no. 10, pp. 1222–1227, 2020, doi: 10.47037/2020.ACES.J.351016.

[15] R. A. Alahnomi, Z. Zakaria, Z. M. Yussof, T. Sutikno, A. A. Mohd Bahar, and A. Alhegazi, "Determination of solid material permittivity using T-ring resonator for food industry," *Telkomnika (Telecommunication Comput. Electron. Control.*, vol. 17, no. 1, pp. 489–496, 2019, doi: 10.12928/TELKOMNIKA.v17i1.11636.

[16] S. Kiani, P. Rezaei, M. Navaei, and M. S. Abrishamian, "Microwave

Sensor for Detection of Solid Material Permittivity in Single/Multilayer Samples With High Quality Factor," *IEEE Sens. J.*, vol. 18, no. 24, pp. 9971–9977, 2018, doi: 10.1109/JSEN.2018.2873544.
[17] B. D. Wiltshire, T. Zarifi, and M. H. Zarifi, "Passive Split Ring Resonator Tag Configuration for RFID-Based Wireless Permittivity Sensing," *IEEE Sens. J.*, vol. 20, no. 4, pp. 1904–1911, 2020, doi: 10.1109/JSEN.2019.2950912.
[18] M. Wagih and J. Shi, "Wireless Ice Detection and Monitoring Using Flexible UHF RFID Tags," *IEEE Sens. J.*, vol. 21, no. 17, pp. 18715–18724, 2021, doi: 10.1109/JSEN.2021.3087326.
[19] C. Gocen and M. Palandoken, "UHF RFID Microwave Sensor Tag Design for an RSSI-Based Machine Learning Assisted Binary Ethanol-Water Mixture Characterization," *IEEE Sens. J.*, vol. 24, no. 1, pp. 262–269, 2024, doi: 10.1109/JSEN.2023.3332106.
[20] D. G. Fang, "Antenna Theory and Microstrip Antennas," *Antenna Theory and Microstrip Antennas*, pp. 1–299, 2017, doi: 10.1201/b10302.
[21] R. Garg, P. Bhartia, I. J. Bahl, and A. Ittipiboon, *Microstrip antenna design handbook*. Artech house, 2001.
[22] G. Ghione and M. Pirola, *Microwave electronics*. 2017. doi: 10.1017/9781316756171.
[23] S. Alam, Z. Zakaria, I. Surjati, N. A. Shairi, M. Alaydrus, and T. Firmansyah, "Dual-Band Independent Permittivity Sensor Using Single-Port with a Pair of U-Shaped Structures for Solid Material Detection," *IEEE Sens. J.*, vol. 22, no. 16, pp. 16111–16119, 2022, doi: 10.1109/JSEN.2022.3191345.
[24] S. Alam *et al.*, "High Stability Single-Port Dual Band Microwave Sensor Based on Interdigital Capacitor Structure with Asymmetry Branch Feedline," *IEEE Access*, vol. 13, no. January, 2025, doi: 10.1109/ACCESS.2025.3538042.
[25] W. J. Wu and G. Wang, "A modified AMC-based antenna sensor for contactless measurement of complex permittivity," *Meas. J. Int. Meas. Confed.*, vol. 206, no. June 2022, p. 112261, 2023, doi: 10.1016/j.measurement.2022.112261.

PIER C SYAH ALAM 2025

ORIGINALITY REPORT

| 17% | 12% | 14% | 4% |
|---|---|---|---|
| SIMILARITY INDEX | INTERNET SOURCES | PUBLICATIONS | STUDENT PAPERS |

PRIMARY SOURCES

| | | |
|---|---|---|
| 1 | essuir.sumdu.edu.ua<br>Internet Source | 1% |
| 2 | Tanveer ul Haq, Cunjun Ruan, Xingyun Zhang, Shahid Ullah, Ayesha Kosar Fahad. "Microwave Sensor Based on Complementary Spiral Resonator with Fitting Equation to Evaluate Dielectric Substrates", 2019 International Conference on Microwave and Millimeter Wave Technology (ICMMT), 2019<br>Publication | 1% |
| 3 | aces-society.org<br>Internet Source | 1% |
| 4 | www.nature.com<br>Internet Source | 1% |
| 5 | Submitted to University of Nottingham<br>Student Paper | 1% |
| 6 | www.researchgate.net<br>Internet Source | 1% |
| 7 | Abel Zandamela, Korbinian Schraml, Suramate Chalermwisutkul, Dirk Heberling, Adam Narbudowicz. "Digital pattern synthesis with a compact MIMO antenna of half-wavelength diameter", AEU - International Journal of Electronics and Communications, 2021<br>Publication | 1% |
| 8 | Ahmed Jamal Abdullah Al-Gburi, Norhanani Abd Rahman, Zahriladha Zakaria, Merih Palandoken. "Detection of Semi-Solid | 1% |

Materials Utilizing Triple-Rings CSRR Microwave Sensor", Sensors, 2023
Publication

| | | |
|---|---|---|
| 9 | pdfs.semanticscholar.org<br>Internet Source | 1 % |
| 10 | Yara A. Kamel, Hesham A. Mohamed, Hala ELsadek, Hadia M. ELhennawy. "RF communication between dual band implantable and on body antennas for biotelemetry application", Scientific Reports, 2025<br>Publication | 1 % |
| 11 | Moein Navaei, Pejman Rezaei, Sina Kiani. "Microwave Split Ring Resonator Sensor for Determination of the Fluids Permittivity with Measurement of Human Milk Samples", Radio Science, 2022<br>Publication | <1 % |
| 12 | Tanveerul Haq, Slawomir Koziel. "Novel Complementary Resonator for Dielectric Characterization of Substrates Based on Permittivity and Thickness", IEEE Sensors Journal, 2023<br>Publication | <1 % |
| 13 | Ameer B. Alsultani, Omer S. Alkhafaf, Ákos Szlávecz, J. Geoffrey Chase, Balázs Benyó. "Design of High Sensitivity Split Ring Resonator Sensor for Invasive Blood Glucose Monitoring", IFAC-PapersOnLine, 2024<br>Publication | <1 % |
| 14 | ijeecs.iaescore.com<br>Internet Source | <1 % |
| 15 | semarakilmu.com.my<br>Internet Source | <1 % |
| 16 | Nilesh Kumar Tiwari, Surya Prakash Singh, M Jaleel Akhtar. "Adulteration detection in | <1 % |

petroleum products using directly loaded coupled-line-based metamaterial-inspired submersible microwave sensor", IET Science, Measurement & Technology, 2020
Publication

| | | |
|---|---|---|
| 17 | Chih-Ying Lin. "Design and implementation of A 24-/60-GHz dual-band monopole meander-line planar CMOS antenna", Microwave and Optical Technology Letters, 07/2012<br>Publication | <1 % |
| 18 | Submitted to Syiah Kuala University<br>Student Paper | <1 % |
| 19 | eprints.utem.edu.my<br>Internet Source | <1 % |
| 20 | Submitted to Flinders University<br>Student Paper | <1 % |
| 21 | Ján Eliaš, Cicely K. Macnamara. "Mathematical Modelling of p53 Signalling during DNA Damage Response: A Survey", International Journal of Molecular Sciences, 2021<br>Publication | <1 % |
| 22 | fortuneonline.org<br>Internet Source | <1 % |
| 23 | www.hindawi.com<br>Internet Source | <1 % |
| 24 | Xueyun Han, Xiaosong Li, Yingping Zhou, Zhongjun Ma, Peidong Peng, Chenghao Fu, Lei Qiao. "Microwave Sensor Loaded With Complementary Curved Ring Resonator (CCRR) for Material Permittivity Detection", IEEE Sensors Journal, 2022<br>Publication | <1 % |
| 25 | pubs.aip.org<br>Internet Source | <1 % |

26 Hussein Jasim, Sadiq Ahmed, Iulia Mocanu, Amer Al-Behadili. "Microstrip Patch Sensor for Characterizing Saline Solution Based on Complimentary Split-Ring Resonators (SC-SRRs)", Sensors, 2025 <1%
Publication

---

27 Remsha Moolat, Manoj Mani, Mohanan Pezholil. "Non-invasive Measurement of Complex permittivity using a Compact Planar Microwave Sensor", 2022 3rd URSI Atlantic and Asia Pacific Radio Science Meeting (AT-AP-RASC), 2022 <1%
Publication

---

28 Teguh Firmansyah, Supriyanto Praptodiyono, Imamul Muttakin, Ken Paramayudha et al. "Multifunctional Glass Microfluidic Microwave Sensor Attenuator for Detection of Permittivity and Conductivity With Device Protection", IEEE Sensors Journal, 2024 <1%
Publication

---

29 Submitted to University Tun Hussein Onn Malaysia <1%
Student Paper

---

30 downloads.hindawi.com <1%
Internet Source

---

31 Ahmed Jamal Abdullah Al-Gburi, Norhanani Abd Rahman, Zahriladha Zakaria, Muhammad Firdaus Akbar. "Realizing the High Q-Factor of a CSIW Microwave Resonator Based on an MDGS for Semisolid Material Characterization", Micromachines, 2023 <1%
Publication

---

32 João G. D. Oliveira, José G. Duarte Junior, Erica N. M. G. Pinto, Valdemir P. Silva Neto, Adaildo G. D'Assunção. "A New Planar Microwave <1%

Sensor for Building Materials Complex Permittivity Characterization", Sensors, 2020
Publication

| | | |
|---|---|---|
| 33 | Merih Palandoken, Cem Gocen. "RFID-Enabled ML-Assisted Microwave Liquid Sensor Design for Complex Dielectric Characterization of Water-Methanol Mixture", Sensors and Actuators A: Physical, 2024<br>Publication | <1 % |

| | | | |
|---|---|---|---|
| Exclude quotes | Off | Exclude matches | < 10 words |
| Exclude bibliography | On | | |